

# Parallel implementation of a lattice-gauge-theory code: studying quark confinement on PC clusters

Attilio Cucchieri, Tereza Mendes, Gonzalo Travieso  
Instituto de Física de São Carlos, Universidade de São Paulo  
C.P. 369, 13560-970 São Carlos, SP, Brazil  
attilio@if.sc.usp.br, mendes@if.sc.usp.br, gonzalo@if.sc.usp.br

Andre R. Taurines  
Instituto de Física, Universidade Federal do Rio Grande do Sul  
Av. Bento Gonçalves, 9500, Campus do Vale, 91501-970 Porto Alegre, RS, Brazil  
taurines@if.ufrgs.br

## Abstract

*We consider the implementation of a parallel Monte Carlo code for high-performance simulations on PC clusters with MPI. We carry out tests of speedup and efficiency. The code is used for numerical simulations of pure  $SU(2)$  lattice gauge theory at very large lattice volumes, in order to study the infrared behavior of gluon and ghost propagators. This problem is directly related to the confinement of quarks and gluons in the physics of strong interactions.*

## 1. Introduction

The strong force is one of the four fundamental interactions of nature (along with gravity, electromagnetism and the weak force). It is the force that holds together protons and neutrons in the nucleus. The strong interaction is described by Quantum Chromodynamics (QCD), a quantum field theory with local  $SU(3)$  gauge invariance [27]. QCD states that a baryon (e.g. a proton or a neutron) is not an elementary particle but is instead made up of building blocks called **quarks**, interacting through the exchange of massless particles called **gluons** (equivalent to the photons in the electromagnetic interaction). A unique feature of the strong force is that the particles that feel it directly — quarks and gluons — are completely hidden from us, i.e. they are never observed as free particles. This property is known as **confinement** and makes QCD much harder to handle theoretically than the theories describing the weak and electromagnetic forces. Indeed, it is not possible to study the confinement problem analytically and physicists must therefore rely on numerical simulations performed on supercomputers. These studies are done using the **lattice** formulation

of QCD [28], which is based on field quantization through Feynman integrals and discretization of space-time on a four-dimensional (Euclidean) lattice. In this formulation — introduced by Wilson in 1974 [32] — the theory becomes equivalent to a model in statistical mechanics and can be studied numerically by Monte Carlo simulations [22]. After over two decades [7] of developments in the methodology for the numerical study of QCD and with present-day computers in the teraflops range, lattice-QCD simulations are now able to provide quantitative predictions with errors of a few percent. This means that these simulations will soon become the main source of theoretical results for comparison with experiments in high-energy physics [15], enabling a much more complete understanding of the physics of the strong force.

The study of lattice QCD constitutes a *Grand Challenge* computational problem [14]. Consequently, lattice-QCD physicists are natural users of high-performance computing and have contributed to the development of supercomputer technology itself. In fact, several research groups have built QCD-dedicated computers, using parallel architecture. Examples are the Hitachi/CP-PACS machine at the University of Tsukuba in Japan [21], the QCDSF and QCDOC machines at Columbia University in the USA [26, 5], and the APE machines [3, 2] at various research centers in Italy and Germany. These computers range from about 1 to 10 teraflops. In addition to these large projects, many groups base their simulations on clusters of workstations or personal computers (PC's) [25], since costs are much lower and maintenance is simpler.

In Brazil, the first PC cluster dedicated to lattice-QCD studies was installed in 2001 at the Physics Department of the University of São Paulo in São Carlos (IFSC-USP), as part of a FAPESP project. The group is currently in-

investigating the behavior of gluon and ghost propagators in Landau gauge [13, 4], with the goal of verifying Gribov's proposed mechanism for quark confinement [19, 33]. This study requires careful consideration of the infrared behavior of these propagators, i.e. their behavior at small momentum  $p$  (typically  $p \ll 1$  GeV). Since the smallest non-zero momentum that can be considered on a lattice is given by  $p_{min} \approx 2\pi/L$  — where  $L$  is the size of the lattice in physical units — it is clear that one needs to simulate at very large lattice sizes in order to probe the small-momentum limit. For example, to have  $p_{min} \approx 0.06$  GeV with a lattice spacing of about 0.17 fm (i.e. physically relevant values for small momentum and fine enough lattice<sup>1</sup>), one needs to simulate on a lattice with 140 sites in each direction. This is considerably more than what can be currently done in QCD simulations. On the other hand, Gribov's predictions are also valid for simpler cases of lattice gauge theories [33], such as three-dimensional two-color QCD with infinitely massive quarks, i.e. (pure)  $SU(2)$  lattice gauge theory in three dimensions. This corresponds to considering the  $SU(2)$  [instead of the  $SU(3)$ ] gauge group [31], taking three (instead of the usual four) space-time dimensions and making the so-called quenched approximation [28]. In this case it was possible to simulate on  $140^3$  lattices and to see clear evidence of Gribov's predicted behavior for the gluon propagator [12]. This represents the largest number of points per direction ever considered in lattice-gauge-theory simulations. The study is currently being extended to even larger lattices (up to  $260^3$ ) aiming at a more quantitative understanding of Gribov's confinement scenario. The consideration of very large lattice sizes requires parallelization and high efficiency of the code in order to obtain good statistics in the Monte Carlo simulation. Thus, an optimized parallel code is of great importance.

The purpose of the present paper is to describe the implementation of the code used in the study above, including a discussion of speedup (at fixed and variable volume) and efficiency. The algorithms for these simulations and their parallelization are briefly reviewed in Section 2. Our PC cluster is described in Section 3, together with the performance of the code. Finally, in Section 4 we comment on the results and report our conclusions.

## 2. The algorithms

Lattice field theories are defined<sup>2</sup> by a functional of the fields — the action  $S[U]$  — which determines the (unrenormalized) statistical weight  $e^{-S[U]}$  of a given field configuration  $\{U\}$ . All quantities of interest, called *observables*,

are computed as weighted averages over the configurations, with the weight function above. For a generic observable  $\mathcal{O}[U]$  this average is defined as

$$\langle \mathcal{O} \rangle \equiv \frac{\sum_U \mathcal{O}[U] e^{-S[U]}}{\sum_U e^{-S[U]}}. \quad (1)$$

In our case  $\{U\}$  is given by the gluon field  $U_\mu(x)$ , which is a matrix defined on each site  $x$  and for each direction  $\mu$  of the lattice. The observables we consider are the gluon and ghost propagators.

The standard Wilson action for  $SU(2)$  lattice gauge theory in  $d$  dimensions is [32]

$$S[U] \equiv \frac{\beta}{2} \sum_{\mu, \nu=1}^d \sum_x \left\{ 1 - \frac{1}{2} \text{Tr} P_{\mu\nu} \right\}, \quad (2)$$

where the plaquette  $P_{\mu\nu}$  is given by the product of the gluon fields  $U_\mu(x)$  around a closed  $1 \times 1$  loop:

$$P_{\mu\nu} \equiv U_\mu(x) U_\nu(x + e_\mu) U_\mu^{-1}(x + e_\nu) U_\nu^{-1}(x). \quad (3)$$

Here,  $U_\mu(x)$  are  $SU(2)$  matrices,  $x$  (with coordinates  $x_\mu = 1, 2, \dots, N_\mu$ ) are sites on a  $d$ -dimensional lattice with periodic boundary conditions and  $e_\mu$  is a unit vector in the positive  $\mu$  direction. The parameter  $\beta$  controls the proximity to the continuum limit. The action in eq. (2) is invariant under the so-called *local gauge transformation*

$$U_\mu(x) \rightarrow U_\mu^{(g)}(x) \equiv g(x) U_\mu(x) g^{-1}(x + e_\mu), \quad (4)$$

where  $g(x)$  are general  $SU(2)$  matrices. Indeed, gauge theories are systems with redundant dynamical variables, which do not represent true dynamical degrees of freedom. This implies that the objects of interest are not the gluon fields  $U_\mu(x)$  themselves, but rather the classes (orbits) of gauge-related fields  $U_\mu^{(g)}(x)$ . The elimination of such redundant gauge degrees of freedom is often essential for understanding and extracting physical information from these theories. This is usually done by a method called **gauge fixing**, in which a unique representative is chosen on each gauge orbit [18].

For an  $SU(2)$  matrix we shall use the parametrization

$$g \equiv g_0 \mathbb{1} + i\vec{\sigma} \cdot \vec{g} = \begin{pmatrix} g_0 + ig_3 & g_2 + ig_1 \\ -g_2 + ig_1 & g_0 - ig_3 \end{pmatrix}, \quad (5)$$

where the components of  $\vec{\sigma} \equiv (\sigma_1, \sigma_2, \sigma_3)$  are the three Pauli matrices [31] and  $\cdot$  stands for scalar product. Then, the adjoint of a matrix  $g \in SU(2)$  is given by

$$g^\dagger = g^{-1} = g_0 \mathbb{1} - i\vec{\sigma} \cdot \vec{g}. \quad (6)$$

Also, note that the unitarity condition  $\det g = 1$  (where  $\det$  indicates the determinant of a matrix) implies  $g_0^2 + g_1^2 +$

<sup>1</sup> We note that 1 fm =  $10^{-13}$  cm is approximately the size of a proton.  
<sup>2</sup> One usually considers units such that  $\hbar = c = 1$ , where  $\hbar$  is the Plank constant and  $c$  is the speed of light in vacuum.

$g_2^2 + g_3^2 = 1$ , namely an  $SU(2)$  matrix can be considered as a four-dimensional unit vector. For the gluon field  $U_\mu(x) \in SU(2)$  one usually writes

$$U_\mu(x) = A_{0,\mu}(x) \mathbb{1} + i\vec{\sigma} \cdot \vec{A}_\mu(x). \quad (7)$$

Our goal is to evaluate numerically the gluon and ghost propagators  $D(k)$  and  $G(k)$ , defined in Section 2.3 [see eqs. (28) and (29)]. To this end one needs to (i) produce a thermalized configuration  $\{U_\mu(x)\}$  by Monte Carlo simulation, (ii) gauge fix this configuration, (iii) evaluate the propagators using the gauge-fixed configuration. These steps are described in detail in Sections 2.1, 2.2, 2.3 and are schematically represented in the code below:

```
main()
{
/* set parameters: beta, number of
configurations NC, number of
thermalization sweeps NT, etc. */
read_parameters();
/* {U} is the link configuration */
set_initial_configuration(U);

for (int c=0; c < NC; c++) {
thermalize(U, NT);
gauge_fix(U, g);
evaluate_propagators(U, D, G);
}
}
```

Note that the gauge-fixing step consists in finding a gauge transformation  $\{g(x)\}$  [see eq. (4)] leading to a given gauge condition. In our case, since we are interested in Gribov's predictions, we employ the so-called **Landau gauge**.

The general setup of our simulations is described in Section 3.

## 2.1. Thermalization

In (dynamic) Monte Carlo simulations [22] the weighted configuration-space average defined in (1) is substituted by a time average over successive realizations (i.e. configurations) of the considered system, which evolves according to a Markov process in the so-called Monte Carlo time. Usually, the system is updated by sweeping over all sites of the lattice and generating a new value for the field at each site based on the conditional probability distribution obtained by keeping all other field variables fixed. In the *heat-bath* update, for example, this single-site distribution is sampled exactly. In QCD simulations one considers only effectively independent field configurations. This means that one follows the system's evolution for a large enough number of time steps such that a statistically independent new configuration is generated, discarding the intermediate steps. Per-

forming the Monte Carlo iterations to obtain such independent field configurations is called *thermalization*.

To thermalize the fields  $\{U_\mu(x)\}$  we use a standard heat-bath algorithm [6] accelerated by *hybrid overrelaxation* [1]. This corresponds to doing  $n$  *micro-canonical* (or energy-conserving) update sweeps over the lattice, followed by one local ergodic update (a heat-bath sweep). As explained below, the micro-canonical sweeps are important for a more efficient sampling of the configuration space. For the heat-bath update, one considers the contribution of a single link variable  $U_\mu(x)$  to the Wilson action (2). This single-link action is given by

$$S_{SL} = -\frac{\beta}{2} \text{Tr} [U_\mu(x) H_\mu(x)] + \text{constant}, \quad (8)$$

where the “effective magnetic field”  $H_\mu(x)$  is defined as

$$H_\mu(x) \equiv \sum_{\nu \neq \mu} [U_\nu(x + e_\mu) U_\mu^{-1}(x + e_\nu) U_\nu^{-1}(x) + U_\nu^{-1}(x - e_\nu + e_\mu) U_\mu^{-1}(x - e_\nu) U_\nu(x - e_\nu)]. \quad (9)$$

Since the matrix  $H_\mu(x)$  is proportional to an  $SU(2)$  matrix, we can write it as

$$H_\mu(x) \equiv \mathcal{N}_\mu(x) \tilde{H}_\mu(x), \quad (10)$$

with  $\tilde{H}_\mu(x) \in SU(2)$  and  $\mathcal{N}_\mu(x) \equiv \sqrt{\det H_\mu(x)}$ . Then, by using the invariance of the group measure under group multiplication, one obtains the heat-bath update [6]

$$U_\mu(x) \rightarrow V \tilde{H}_\mu^{-1}(x), \quad (11)$$

where the  $SU(2)$  matrix  $V = v_0 \mathbb{1} + i\vec{\sigma} \cdot \vec{v}$  must be generated by choosing  $v_0$  according to the distribution

$$\sqrt{1 - v_0^2} \exp[\beta \mathcal{N}_\mu(x) v_0] dv_0 \quad (12)$$

and the vector  $\vec{v}$  (which is normalized to  $\sqrt{1 - v_0^2}$ ) pointing along a uniformly chosen random direction in three-dimensional space.

The vector  $\vec{v}$  can be easily generated. For example, if we use cylindrical coordinates we may take

$$v_1 = \sqrt{(1 - \rho^2)(1 - v_0^2)} \cos \phi \quad (13)$$

$$v_2 = \sqrt{(1 - \rho^2)(1 - v_0^2)} \sin \phi \quad (14)$$

$$v_3 = \sqrt{1 - v_0^2} \rho \quad (15)$$

with  $\rho$  uniformly distributed in  $[-1, 1]$  and  $\phi$  uniformly distributed in  $[0, 2\pi]$ . On the contrary, the problem of generating  $v_0$  according to the distribution (12) is considerably more involved. Three different rejection methods for this purpose are considered in [17, Appendix A]. Here, we use their algorithms called method 1 and method 2, with a cut-off value of 2.0 for the quantity  $\beta \mathcal{N}_\mu(x)$ , namely method 1

is used when  $\beta \mathcal{N}_\mu(x) < 2.0$  and method 2 is used otherwise.

In order to implement the heat-bath method one also needs a (parallelized) random number generator. Here we adopt the RANLUX generator, which is based on chaos theory [24]. More precisely, we use a double-precision implementation of RANLUX (version 2.1) with luxury level set to 2.

Let us now consider the (deterministic) micro-canonical update, used in the hybrid overrelaxed algorithm:

$$U_\mu(x) \rightarrow \tilde{H}_\mu^{-1}(x) \text{Tr} \left[ U_\mu(x) \tilde{H}_\mu(x) \right] - U_\mu(x). \quad (16)$$

From formulae (8) and (10) it is easy to see that this update does not change the value of the action  $S_{SL}$ . On the other hand, the step in (16) represents a large move in configuration space [1]. Thus, one can alternate micro-canonical sweeps of the lattice and heat-bath updates in order to reduce the problem of critical slowing-down, which afflicts Monte Carlo simulations of critical phenomena [30]. The efficiency of the hybrid overrelaxed algorithm may be optimized by tuning the value of  $n$ , i.e. the number of micro-canonical sweeps between two heat-bath sweeps.

## 2.2. Landau gauge fixing

For a given thermalized lattice configuration  $\{U_\mu(x)\}$ , Landau gauge fixing is obtained by looking for a gauge transformation  $\{g(x) \in SU(2)\}$  that brings the functional

$$\mathcal{E}_V[g] \equiv - \sum_{\mu=1}^d \sum_x \text{Tr} \left[ g(x) U_\mu(x) g^\dagger(x + e_\mu) \right] \quad (17)$$

to a local minimum, starting from randomly chosen  $\{g(x)\}$  [18]. Thus, from the numerical point of view, fixing the lattice Landau gauge is a minimization problem. Here, we consider three different (iterative) gauge-fixing algorithms [8, 9]: the so-called *Cornell* (COR) method, the *stochastic overrelaxation* (SOR) algorithm and the *Fourier acceleration* (FA) algorithm. Let us notice that the first two algorithms are based on local updates for the matrices  $g(x)$  and have dynamic critical exponent  $z = 1$ . This means that the number of iterations required to achieve a given accuracy in the minimization of the functional  $\mathcal{E}_V[g]$  grows as a function of the lattice side  $N$  as  $N^{d+1}$ , when considering a symmetric lattice in  $d$  dimensions. On the other hand, the FA algorithm is based on a global update and has  $z = 0$  [at least for sufficiently smooth field configurations  $\{U_\mu(x)\}$ ]. Its computational work grows roughly as  $N^d$ . Thus, even though the CPU time necessary to update a single-site variable  $g(x)$  is much smaller for the two local methods than for the FA method, the latter should clearly be used when considering very large values of  $N$ .

The update  $g(x) \rightarrow g_{new}(x)$  for the COR and the SOR methods can be written in terms of local quantities — i.e. quantities defined only in terms of the site  $x$  — and of the matrix

$$h(x) \equiv \sum_{\mu=1}^d \left[ U_\mu(x) g^\dagger(x + e_\mu) + U_\mu^\dagger(x - e_\mu) g^\dagger(x - e_\mu) \right]. \quad (18)$$

On the contrary, for the FA method one needs to evaluate

$$\vec{u}(x) = \left[ (-\Delta)^{-1} \vec{w} \right](x), \quad (19)$$

where  $w(x) \equiv g(x)h(x)$ , the three-dimensional vector  $\vec{w}$  is given by [see eq. (5)]

$$2i \vec{\sigma} \cdot \vec{w}(x) \equiv w(x) - w^\dagger(x) \quad (20)$$

and  $-\Delta$  is (minus) the lattice Laplacian, defined for a general vector field  $\vec{f}(x)$  as

$$\left( -\Delta \vec{f} \right)(x) \equiv \sum_{\mu=1}^d \left[ 2\vec{f}(x) - \vec{f}(x + e_\mu) - \vec{f}(x - e_\mu) \right]. \quad (21)$$

From eq. (19) it is evident that the FA method is actually a Laplacian preconditioning algorithm.

Traditionally the inversion of the lattice Laplacian is done using a fast Fourier transform (FFT), after writing

$$\left( -\Delta \right)^{-1} = \hat{F}^{-1} \frac{1}{p^2} \hat{F}, \quad (22)$$

where  $\hat{F}$  indicates the Fourier transform,  $\hat{F}^{-1}$  is its inverse and  $p^2$  is the squared magnitude of the lattice momentum. Alternatively [10], the inversion of the Laplacian may be done using a multigrid (MG) algorithm or a conjugate gradient (CG) method, avoiding the use of the FFT, which has high communication costs in a parallel implementation. Indeed, one obtains [10, 11] the same convergence as for the original algorithm (based on FFT), when using an accuracy of about  $10^{-3}$  for the MG or CG (iterative) inversion. At the same time, the computational cost of the new implementations is smaller than that of the FFT-FA method when considering large lattice volumes. This is true even for a non-parallelized code. Moreover, the MG-FA and CG-FA algorithms are well suited for vector and parallel machines and they make the FA method more flexible, i.e. it works equally well with any lattice side.<sup>3</sup> Here we do the inversion of the Laplacian using a CG method preconditioned with red/black ordering [16]. As stopping criterion we consider  $r_t/r_0 \leq 10^{-3}$ , where  $r_t$  is the magnitude of the CG

<sup>3</sup> We note that the FFT is slightly less efficient for lattice sides  $N$  that are not powers of 2 [34].

residual after  $t$  iterations. We note that, with this stopping criterion, one can do the inversion in single precision, even though the rest of the code is written in double precision. This corresponds to a speed-up of almost a factor 2 in the inversion.

Let us stress that the three algorithms considered above require the tuning of a free parameter in order to attenuate critical slowing-down, or equivalently in order to reduce the computational work. Notice however that the CPU time necessary to update a single-site variable  $g(x)$  is essentially independent of the value of the tuning parameter.

**2.2.1. Convergence of the gauge fixing** Several quantities have been introduced in order to check the convergence of Landau-gauge-fixing algorithms [8]. We consider here

$$(\nabla A)^2 \propto \sum_x \sum_{b=1}^3 \left[ (\nabla \cdot A_b)(x) \right]^2, \quad (23)$$

which is commonly used in numerical simulations, and

$$\Sigma_Q \equiv \frac{1}{d} \sum_{\mu=1}^d \frac{1}{3N_\mu} \sum_{b=1}^3 \sum_{x_\mu=1}^{N_\mu} \frac{[Q_{b,\mu}(x_\mu) - \bar{Q}_{b,\mu}]^2}{[\bar{Q}_{b,\mu}]^2}, \quad (24)$$

which provides a very sensitive test of the goodness of the gauge fixing. Let us recall that

$$(\nabla \cdot A_b)(x) \equiv \sum_{\mu=1}^d [A_{b,\mu}(x) - A_{b,\mu}(x - e_\mu)] \quad (25)$$

is the lattice divergence of  $A_{b,\mu}(x)$  [see eq. (7)]. We also define

$$\bar{Q}_{b,\mu} \equiv \frac{1}{N_\mu} \sum_{x_\mu=1}^{N_\mu} Q_{b,\mu}(x_\mu), \quad (26)$$

where the quantities

$$Q_{b,\mu}(x_\mu) \equiv \sum_{\nu \neq \mu} \sum_{x_\nu} A_{b,\mu}(x) \quad \mu = 1, \dots, d \quad (27)$$

are constant (i.e. independent of  $x_\mu$ ) if the Landau-gauge-fixing condition is satisfied. The two quantities  $(\nabla A)^2$  and  $\Sigma_Q$  are expected to converge to zero exponentially (and with the same exponent) as a function of the number of gauge-fixing sweeps, even though their sizes may differ considerably.

### 2.3. Evaluation of the propagators

A propagator of a field is a two-point function, i.e. a correlation function between values of the field at two different points in space-time [23]. In quantum mechanics, the propagator determines the evolution of the wave function of a system and, for a particle, it gives the probability amplitude

of going (i.e. propagating) from a point in space-time to another [29]. More generally, Green's functions (i.e.  $n$ -point functions) carry all the information about the physical and mathematical structure of a quantum field theory. From this point of view, two-point functions (propagators) are a theory's most basic quantities and the gluon propagator may be thought of as the most basic quantity of QCD. The ghost propagator appears in the theory as a consequence of the gauge-fixing procedure described above.

The gluon propagator is conveniently defined in momentum space as

$$D(k) \propto \sum_{\mu,b} \langle \left| \sum_x A_{b,\mu}(x) \exp(2\pi i k \cdot x) \right|^2 \rangle. \quad (28)$$

Here,  $b$  goes from 1 to 3 [when considering the  $SU(2)$  gauge group],  $\mu$  goes from 1 to  $d$  ( $d = 3$  for three-dimensional space-time),  $k$  has components  $k_\mu$  taking values  $k_\mu N_\mu = 0, 1, \dots, N_\mu - 1$  and the field  $A_{b,\mu}(x)$  is defined in eq. (7). Note that  $\cdot$  stands for scalar product and  $|\dots|$  indicates the norm of a complex number.

The numerical evaluation of the ghost propagator (in momentum space) is considerably more involved. In fact, one has to calculate

$$G(k) \propto \sum_{x,y} e^{-k \cdot (x-y)} \sum_b \langle (\mathcal{M}^{-1})_{bb}(x,y;U) \rangle, \quad (29)$$

where the matrix  $\mathcal{M}_{ab}(x,y;U)$  is a sparse matrix that depends on the gluon field  $U_\mu(x)$ . (For an explicit definition of this matrix see eq. (B.18) in [33].) Note that, since the color indices  $a$  and  $b$  go from 1 to 3 [for the  $SU(2)$  group] and if there are  $N^d$  lattice sites, the size of this matrix is  $3N^d \times 3N^d$ .

The inversion of the matrix  $\mathcal{M}_{ab}(x,y;U)$  can be done using a CG method with red/black ordering, as in the case of the lattice Laplacian considered above for gauge fixing. This part of our code has not been parallelized yet, but we expect to obtain a speedup comparable to the one obtained for the lattice-Laplacian case.

### 2.4. Parallelization

As said above, we need a parallelized code in order to simulate at very large lattice sizes. We have started by considering the QCDMP I package [35], which is based on the work of Hioki [20]. The advantages of this package are its portability and the efficient way of evaluating the effective magnetic field  $H_\mu(x)$  — also called the *staple* — defined in eq. (9). In particular, the extra memory space required for communication is considerably reduced with respect to previous implementations. The original QCDMP I code is written for pure  $SU(3)$  lattice gauge theory in  $d$  dimensions ( $d \geq 2$ ) and performs only the (heat-bath) thermalization step of the simulation. We have adapted the original code

to the  $SU(2)$  case and improved the generation of  $v_0$  according to the distribution (12). More precisely (see Section 2.A), we have added method 1 and a more efficient version of method 2. At the same time, we have introduced the micro-canonical step, the various Landau-gauge-fixing algorithms discussed in Section 2.B (i.e. the COR, SOR and CG-FA methods), the calculation of the quantities  $(\nabla A)^2$  and  $\Sigma_Q$  for checking the convergence of the gauge fixing, and the evaluation of the gluon propagator. (As mentioned above, we have not yet parallelized the evaluation of the ghost propagator.)

For the parallelization, we divide the lattice equally among the nodes, i.e. we place  $v = V/M$  sites of the lattice in each node, where  $V$  is the lattice volume and we use  $M$  nodes. Each node gets a contiguous block of lattice sites. We will refer to this block of sites as the *local lattice* in a node. Note that, in general, not all directions  $\mu$  of the lattice are divided between different nodes and that, in order to use a red/black ordering, the number of sites  $v$  in each node must be even.

Let us stress that communication is required for the evaluation of the staple  $H_\mu(x)$ , for the calculation of  $h(x)$  [see eq. (18)] and (in the CG-FA method) for the inversion of the lattice Laplacian [see eq. (21)]. Also, the evaluation of the quantities  $(\nabla A)^2$  and  $\Sigma_Q$  (see Section 2.B.1) requires some level of communication in a parallel code, while for the gluon propagator [see eq. (28)] one has to perform only a sum over the whole lattice. Since the expressions to be parallelized involve at most quantities at lattice sites that are nearest neighbors, communication is required only for sites on the boundary of the local lattice in a node. Moreover, simulations are usually done in three or four dimensions, leading to a high granularity due to the surface/volume effect.

All communications in [20] are carried out using just two subroutines. The first (called `setlink`) sends data from a node to the previous one in a given direction. The second subroutine (called `slidematrix`) sends data from a node to the next one (in a given direction). Clearly, these two routines are all we need in order to perform the communications required in our code.

### 3. Performance

As mentioned in the Introduction, our simulations were done on a PC cluster at the IFSC-USP. The system has 16 nodes and a server, all with 866 MHz Pentium III CPU. The nodes have 256 MB RAM memory (working at 133 MHz) and the operating system is Debian GNU/Linux (version 3.0r0). The machines are connected with a 100 Mbps full-duplex network through a 3COM switch. All user directories are located on the server, which has two SCSI disks,

and are mounted by the nodes (using NFS). The server is not used for the computations.

Our code (as well as the QCDMPI package) is written in FORTRAN 77 making use of MPI for communication. The code may be run for a general lattice dimension  $d \geq 2$ . As said before, we consider here  $d = 3$ . We use MPICH (version 1.2.1-16) and the compiler `g77` (version 0.5.24). The compilation has been done with the following four options `-march=pentiumpro -fomit-frame-pointer -mpreferred-stack-boundary=2 -O3`.

Table 1: Average CPU-time (in  $\mu s$ ) to update a link variable  $U_\mu(x)$  using heat-bath ( $t_{hb}$ ) or micro-canonical update ( $t_{mc}$ ). Errors are one standard deviation.

$M$	Node topol.	$t_{hb}$	$t_{mc}$
1	$1 \times 1 \times 1$	10.341(4)	6.0190(1)
2	$2 \times 1 \times 1$	5.6(2)	3.2099(4)
4	$2 \times 2 \times 1$	2.78(2)	1.6958(3)
4	$4 \times 1 \times 1$	2.898(6)	1.817(3)
8	$2 \times 2 \times 2$	1.435(7)	0.8881(3)
8	$4 \times 2 \times 1$	1.48(2)	0.9125(6)
8	$8 \times 1 \times 1$	1.9(1)	1.236(4)
16	$4 \times 2 \times 2$	0.758(7)	0.4732(3)
16	$4 \times 4 \times 1$	0.75(1)	0.4614(4)
16	$8 \times 2 \times 1$	0.849(8)	0.5677(3)
16	$16 \times 1 \times 1$	1.25(1)	0.6735(5)

We now describe the setup of a complete simulation. As said in Section 2.A, we generate statistically independent field configurations to be used for the evaluation of the Monte Carlo average of an observable, which provides an estimate of the average in eq. (1). In order to reduce the statistical error (i.e. the Monte Carlo error) of this estimate, one typically needs to produce hundreds of such configurations. For each of them there are two computational steps involved: the Monte Carlo generation of a new independent field configuration and the evaluation of the desired observables. The first step is the thermalization, which in our case is done using the hybrid overrelaxed algorithm. This usually requires hundreds of sweeps of the lattice, corresponding to several hours to produce a new configuration. The second step is often even more time-consuming. In our case the evaluation of the observables (i.e. the propagators) is done only after the new configuration has been gauge-fixed, by an iterative minimization procedure. One usually needs thousands of iterations in order to reach a prescribed accuracy (for example  $\Sigma_Q \leq 10^{-12}$ , required for a good quality of the gauge fixing). The actual computation of the gluon propagator requires a negligible time. (This is not true for the ghost propagator.) Consequently, for typical values

of lattice volumes, a complete simulation may take several months. For example, in order to produce the (preliminary) data reported in [12], the code was running on our PC cluster for almost three months. The production of the corresponding final results is expected to take almost one year of runs. As an illustration, for  $V = 140^3$  and  $\beta = 6.0$  the average CPU-times (per configuration) using 4 nodes are: about 8 hours for thermalization and about 21 hours for gauge fixing (using COR or SOR methods). We note that the total CPU-time per configuration is not appreciably affected by changes in the parameter  $\beta$ . [More precisely, for smaller (respectively larger) values of  $\beta$  one spends a little less (resp. more) time for thermalization and a little more (resp. less) time for gauge fixing.] We plan to use the CG-FA method in future production runs, to reduce the percentage of time spent in gauge fixing.

We report below on some runs performed for testing the speedup and efficiency of our code.

### 3.1. Speedup at fixed volume

We did tests for the various algorithms, considering a fixed lattice volume  $V = 64^3$ , using 1, 2, 4, 8 and 16 nodes. Let us note that this lattice size is relatively small. In fact, it can be simulated on a single node (without parallelization) using less than 20% of the memory (about 24% if one employs the CG-FA method for gauge fixing). Thus, since communications are proportional to the surface area of the local lattice in a node, these tests correspond to a worse situation than the one we considered for our production runs in [12].

In Tables 1 and 2 we report the average CPU-time (in micro-seconds) necessary to update a link variable  $U_\mu(x)$  using a heat-bath ( $t_{hb}$ ) or a micro-canonical update ( $t_{mc}$ ), and the time to update a site variable  $g(x)$  using the gauge-fixing methods COR ( $t_{cor}$ ), SOR ( $t_{stoc}$ ) or CG-FA ( $t_{cg}$ ). These CPU-times are given for different values of the number of nodes  $M$  and different (three-dimensional) node topology.

### 3.2. Speedup at variable volume

We also did tests at variable volume, considering five different node topologies:  $1 \times 1 \times 1$ ,  $1 \times 1 \times 2$ ,  $1 \times 2 \times 2$ ,  $2 \times 2 \times 2$  and  $2 \times 2 \times 4$ , corresponding respectively to  $M = 1, 2, 4, 8$  and 16 nodes. For each node topology we have simulated using three different lattice volumes  $V$ . Results of these tests are reported in Tables 3 and 4 for different numbers of nodes  $M$  and for the various lattice volumes. As can be seen from the first two columns in these tables, the lattice volumes have been chosen so that the local lattice volume  $v = V/M$  is always given by one of the following cases:  $4^3$ ,  $16^3$  and  $64^3$ . Let us note that this arrange-

Table 2: Average CPU-time (in  $\mu s$ ) to update a site variable  $g(x)$  using gauge-fixing methods COR ( $t_{cor}$ ), SOR ( $t_{stoc}$ ) or CG-FA ( $t_{cg}$ ). Errors are one standard deviation.

$M$	Node topol.	$t_{cor}$	$t_{stoc}$	$t_{cg}$
1	$1 \times 1 \times 1$	5.606(2)	6.272(2)	253(1)
2	$2 \times 1 \times 1$	2.9659(7)	3.295(1)	136.2(2)
4	$2 \times 2 \times 1$	1.560(1)	1.7232(5)	70.9(3)
4	$4 \times 1 \times 1$	1.6063(5)	1.789(1)	73.6(3)
8	$2 \times 2 \times 2$	0.819(1)	0.9011(4)	37.5(1)
8	$4 \times 2 \times 1$	0.833(1)	0.9175(7)	37.2(1)
8	$8 \times 1 \times 1$	1.0228(5)	1.1133(4)	43.5(1)
16	$4 \times 2 \times 2$	0.4383(3)	0.4771(2)	18.99(5)
16	$4 \times 4 \times 1$	0.4315(4)	0.4706(1)	18.43(5)
16	$8 \times 2 \times 1$	0.4870(6)	0.5296(2)	19.22(6)
16	$16 \times 1 \times 1$	0.5924(4)	0.644(3)	27.29(5)

ment is closer to what is usually considered for production runs. In fact, when carrying out parallel simulations at increasingly large lattice volumes on a PC cluster, it is preferable to fill up the memory in each node before increasing the number of nodes. (This reduces the percentage of time spent in communication.)

Table 3: Average CPU-time (in  $\mu s$ ) to update a link variable  $U_\mu(x)$  using heat-bath ( $t_{hb}$ ) or micro-canonical update ( $t_{mc}$ ). Errors are one standard deviation.

$M$	$V$	$t_{hb}$	$t_{mc}$
1	$4^3$	4.76(1)	1.028(2)
1	$16^3$	8.05(6)	4.1821(9)
1	$64^3$	10.383(5)	6.0186(1)
2	$4^2 \times 8$	9.19(2)	7.08(1)
2	$16^2 \times 32$	4.9(1)	2.7561(9)
2	$64^2 \times 128$	5.39(7)	3.1184(2)
4	$4 \times 8^2$	8.1(2)	7.4(3)
4	$16 \times 32^2$	2.708(9)	1.6940(9)
4	$64 \times 128^2$	2.768(3)	1.6175(3)
8	$8^3$	5.94(8)	5.02(6)
8	$32^3$	1.54(2)	1.0090(2)
8	$128^3$	1.55(8)	0.8447(3)
16	$8^2 \times 16$	5.8(6)	4.4(2)
16	$32^2 \times 64$	0.763(2)	0.5111(3)
16	$128^2 \times 256$	0.77(1)	0.436(1)

Table 4: Average CPU-time (in  $\mu s$ ) to update a site variable  $g(x)$  using gauge-fixing methods COR ( $t_{cor}$ ), SOR ( $t_{stoc}$ ) or CG-FA ( $t_{cg}$ ). Errors are one standard deviation.

$M$	$V$	$t_{cor}$	$t_{stoc}$	$t_{cg}$
1	$4^3$	1.21(7)	1.60(1)	4.26(3)
1	$16^3$	3.90(1)	4.224(6)	19.82(4)
1	$64^3$	5.606(2)	6.272(2)	253(1)
2	$4^2 \times 8$	6.41(8)	6.79(4)	117.2(6)
2	$16^2 \times 32$	2.413(5)	2.679(4)	31.38(6)
2	$64^2 \times 128$	2.885(1)	3.2329(4)	122(3)
4	$4 \times 8^2$	6.2(2)	6.10(6)	125.1(2)
4	$16 \times 32^2$	1.497(3)	1.571(3)	26.47(5)
4	$64 \times 128^2$	1.4935(2)	1.6634(3)	63.7(7)
8	$8^3$	4.53(6)	4.64(5)	96.1(9)
8	$32^3$	0.862(2)	0.927(1)	18.83(8)
8	$128^3$	0.7620(2)	0.8528(1)	31.5(2)
16	$8^2 \times 16$	3.56(7)	4.4(2)	89.6(7)
16	$32^2 \times 64$	0.4496(7)	0.480(1)	14.25(4)
16	$128^2 \times 256$	0.3942(3)	0.4385(2)	17.6(5)

#### 4. Results and conclusions

The CPU-times reported above indicate that the parallelization is rather good for the five algorithms considered (the heat-bath and micro-canonical methods for thermalization, and the COR, SOR and CG-FA methods for gauge fixing). Also, the values for the speedup  $S = t_1/t_M$  (and the efficiency  $E = S/M$ ) are very similar for the five cases. We therefore take averages over the five methods and report them in Table 5. In the fixed-volume case we present results for node topologies  $2 \times 2 \times 1$ ,  $2 \times 2 \times 2$  and  $4 \times 4 \times 1$  respectively for the cases  $M = 4, 8$  and  $16$ . (This corresponds to the best performance for a given number of nodes.) In the variable-volume case we consider results obtained using the largest lattice volume for each node topology. We clearly see that one obtains a good parallelization even in the fixed-volume case and using a relatively small lattice volume  $V$ . Indeed, the efficiency decreases slowly when doubling the number of nodes and it is still about 0.84 at  $M = 16$ . As expected, the performance is better for the variable-volume case when considering large values of the local lattice volume  $v$  in a node. As said above, this test is closer to the situation usually considered in production runs, with local lattice sizes using more than 50% of the memory of each node.

The data for the speedup at variable volume reported in Table 5 are well fitted by the function  $S(M) = M(1 - c \log M)$  with  $c = 0.038 \pm 0.001$ . The corresponding plot is shown in Figure 1. This would mean a speedup of almost 400 for 512 nodes.

Note that the efficiency loss in going from 1 to  $M$  nodes

Table 5: Average speedup and efficiency.

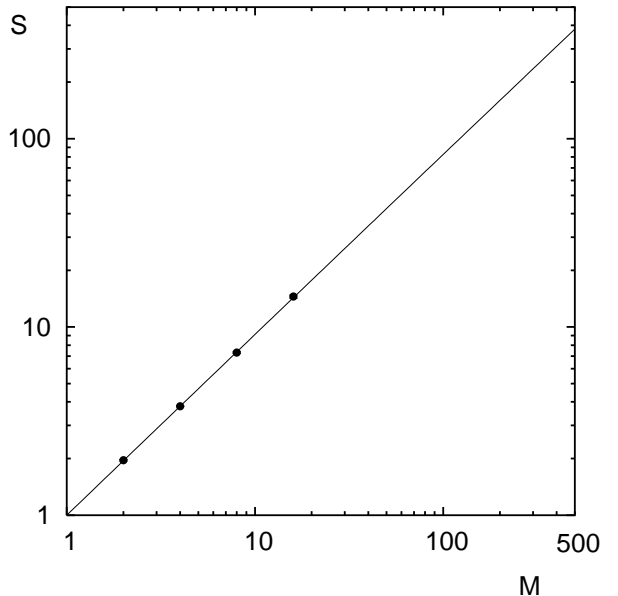
	Fixed volume		Variable volume	
	$S$	$E$	$S$	$E$
1 $\rightarrow$ 2	1.87(2)	0.937(8)	1.96(2)	0.981(8)
1 $\rightarrow$ 4	3.61(1)	0.904(3)	3.79(1)	0.948(3)
1 $\rightarrow$ 8	6.91(2)	0.863(2)	7.31(8)	0.91(1)
1 $\rightarrow$ 16	13.38(6)	0.836(3)	14.5(3)	0.88(1)

at variable volume  $V$  and small  $v$  is due to the effect of node communication over the usage of the cache memory.

We conclude that the parallelization of our code works very well and that simulations of this type are very viable on a PC cluster. Let us point out again the main results of the parallel implementation described in this paper. We have adapted and extended the package QCDMPI, which shows good parallelization but performs only thermalization of the gluon fields. The resulting code employs a more efficient thermalization algorithm and also performs gauge fixing and evaluation of propagators, with essentially the same parallel performance as the original package.

For the future we plan to (i) parallelize the codes for the evaluation of the ghost propagator and for the MG-FA gauge-fixing method, (ii) improve the usage of the cache memory and (iii) introduce overlap of computation and communication.

Figure 1: Code speedup  $S$  at variable volume as a function of the number of nodes  $M$ .



## Acknowledgements

We thank Martin Lüscher for sending us the latest version of the random number generator RANLUX. The research of A.C. and T.M. is supported by FAPESP (Project No. 00/05047-5). A.T. thanks CNPq for financial support.

## References

- [1] S. L. Adler. Algorithms for pure gauge theory. *Nucl. Phys. Proc. Suppl.*, 9:437–446, 1989.
- [2] R. Ammendola et al. Status of the apeNEXT project. <http://arXiv.org/abs/hep-lat/0211031>.
- [3] A. Bartoloni et al. An overview of the APE mille project. *Nucl. Phys. Proc. Suppl.*, 60A:237–240, 1998.
- [4] J. C. R. Bloch, A. Cucchieri, K. Langfeld, and T. Mendes. Running coupling constant and propagators in  $SU(2)$  Landau gauge. *Nucl. Phys. Proc. Suppl.*, 119B:736–738, 2003.
- [5] P. A. Boyle, C. Jung, and T. Wettig. The QCDOC supercomputer: hardware, software, and performance. <http://arXiv.org/abs/hep-lat/0306023>.
- [6] M. Creutz. Monte Carlo study of quantized  $SU(2)$  gauge theory. *Phys. Rev.*, D21:2308–2315, 1980.
- [7] M. Creutz. The early days of lattice gauge theory. <http://arXiv.org/abs/hep-lat/0306024>.
- [8] A. Cucchieri and T. Mendes. Critical slowing-down in  $SU(2)$  Landau gauge-fixing algorithms. *Nucl. Phys.*, B471:263–292, 1996.
- [9] A. Cucchieri and T. Mendes. Study of critical slowing-down in  $SU(2)$  Landau gauge fixing. *Nucl. Phys. Proc. Suppl.*, B53:811–814, 1997.
- [10] A. Cucchieri and T. Mendes. A multigrid implementation of the Fourier acceleration method for Landau gauge fixing. *Phys. Rev.*, D57:R3822–R3826, 1998.
- [11] A. Cucchieri and T. Mendes. Critical slowing-down in  $SU(2)$  Landau-gauge-fixing algorithms at  $\beta = \infty$ . *Comput. Phys. Commun.*, 154(1):1–48, 2003.
- [12] A. Cucchieri, T. Mendes, and A. R. Taurines.  $SU(2)$  Landau gluon propagator on a  $140^3$  lattice. *Phys. Rev.*, D67:R091502, 2003.
- [13] A. Cucchieri, T. Mendes, and D. Zwanziger.  $SU(2)$  running coupling constant and confinement in minimal Coulomb and Landau gauges. *Nucl. Phys. Proc. Suppl.*, B106:697–699, 2002.
- [14] D. E. Culler, J. P. Singh, and A. Gupta. *Parallel computer architecture: a hardware/software approach*. Morgan Kaufmann, San Francisco, CA, 1999.
- [15] C. T. H. Davies et al. High-precision lattice QCD confronts experiment. <http://arXiv.org/abs/hep-lat/0304004>.
- [16] J. J. Dongarra, I. S. Duff, D. C. Sorensen, and H. A. van der Vorst. *Solving linear systems on vector and shared memory computers*. SIAM, Philadelphia, PA, 1991.
- [17] R. G. Edwards, S. J. Ferreira, J. Goodman, and A. D. Sokal. Multigrid Monte Carlo. 3. Two-dimensional  $O(4)$  symmetric nonlinear sigma model. *Nucl. Phys.*, B380:621–664, 1992.
- [18] L. Giusti, M. L. Paciello, C. Parrinello, S. Petrarca, and B. Taglienti. Problems on lattice gauge fixing. *Int. J. Mod. Phys.*, A16:3487–3534, 2001.
- [19] V. N. Gribov. Quantization of non-Abelian gauge theories. *Nucl. Phys.*, B139:1–32, 1978.
- [20] S. Hioki. Construction of staples in lattice gauge theory on a parallel computer. *Parallel Comput.*, 22(10):1335–1344, 1996.
- [21] K. Kanaya. Elementary particles on a dedicated parallel computer. *Fortsch. Phys.*, 50:531–537, 2002.
- [22] D. P. Landau and K. Binder. *A guide to Monte Carlo simulations in statistical physics*. Cambridge University Press, Cambridge, 2000.
- [23] M. Le Bellac. *Quantum and statistical field theory*. Oxford University Press, Oxford, 1995.
- [24] M. Lüscher. A portable high quality random number generator for lattice field theory simulations. *Comput. Phys. Commun.*, 79:100–110, 1994.
- [25] M. Lüscher. Lattice QCD on PCs? *Nucl. Phys. Proc. Suppl.*, B106:21–28, 2002.
- [26] R. D. Mawhinney. The 1 teraflops QCDSPP computer. *Parallel Comput.*, 25:1281–1299, 1999.
- [27] K. Moriyasu. *An elementary primer for gauge theory*. World Scientific, Singapore, 1983.
- [28] H. J. Rothe. *Lattice gauge theories: an introduction*. World Scientific, Singapore, 1987.
- [29] J. J. Sakurai. *Modern quantum mechanics*. Addison-Wesley, Boston, MA, (edited by San Fu Tuan) 2nd edition, 1994.
- [30] A. D. Sokal. Monte Carlo methods in statistical mechanics: foundations and new algorithms. Cargèse 1996, Integration: basics and applications, <http://citeseer.nj.nec.com/sokal96monte.html>.
- [31] W.-K. Tung. *Group theory in physics*. World Scientific, Singapore, 1985.
- [32] K. G. Wilson. Confinement of quarks. *Phys. Rev.*, D10:2445–2459, 1974.
- [33] D. Zwanziger. Fundamental modular region, Boltzmann factor and area law in lattice gauge theory. *Nucl. Phys.*, B412:657–730, 1994.
- [34] <http://www.fft.org/benchfft/results/pii-300-single.html>.
- [35] <http://insam.sci.hiroshima-u.ac.jp/qcdmpi/>.